Hierarchical Multi-Response Gaussian Processes for Uncertainty Analysis with Multi-Scale Composite Manufacturing Simulation

Kai Zhou
Research Assistant Professor
Department of Mechanical Engineering-Engineering Mechanics
Michigan Technological University

Ryan Enos
Graduate Research Assistant
School of Aeronautics and Astronautics Engineering
Purdue University

Dong Xu
Graduate Research Assistant
Department of Mechanical Engineering
University of Connecticut

Dianyun Zhang[†]
Assistant Professor
School of Aeronautics and Astronautics Engineering
Purdue University

Jiong Tang[†]
United Technologies Corporation Professor of Advanced Materials and Processing
Department of Mechanical Engineering
University of Connecticut

[†] Corresponding author:
Dianyun Zhang (dianyun@purdue.edu)
Jiong Tang (jiong.tang@uconn.edu)

Hierarchical Multi-Response Gaussian Processes for Uncertainty Analysis with Multi-Scale of Composite Manufacturing Simulation

Kai Zhou[a], Ryan Enos[b], Dong Xu[c], Dianyun Zhang[b†], Jiong Tang[c†]

a: Department of Mechanical Engineering-Engineering Mechanics, Michigan Technological University

b: School of Aeronautics and Astronautics Engineering, Purdue University

c: Department of Mechanical Engineering, University of Connecticut

ABSTRACT

Variations of constituent fiber and matrix properties and process conditions can cause significant variability in composite parts and affect their performance. The focus of this paper is to establish a new computational framework that can efficiently quantify the uncertainty propagation of parts manufactured through the resin transfer molding (RTM) process. RTM involves a sequence of inter-related processes that span multiple spatial and temporal scales. This calls for a multi-scale analysis for the nominal process, which is computationally complex and intensive. A direct Monte Carlo simulation of uncertainty quantification leads to prohibitive cost. In this research we leverage a sequentially architected multi-response Gaussian process (MRGP) meta-modelling approach to facilitate a hierarchical procedure. This can dramatically reduce the computational cost, and allow us to characterize the process outputs of interest at different scales and at the same time capture the intrinsic correlation amongst these outputs. Moreover, integrating a global sensitivity analysis with the hierarchical MRGP meta-models yields the importance ranking of uncertainty propagation paths. This computational framework provides a quantitative assessment tool of the uncertainties in composite manufacturing. Case study on curing-induced dimensional variability of a curved composite part is conducted for demonstration and validation.

Keywords: uncertainty propagation analysis, resin transfer molding (RTM) process, multi-scale simulation, multi-response Gaussian process (MRGP), global sensitivity analysis, importance ranking.

1. Introduction

Fiber-reinforced composites are increasingly used in aerospace and automobile industries due to their high strength, light weight and easily-tailored mechanical properties. The manufacturing of these composite

† Corresponding author
Dianyun Zhang (dianyun@purdue.edu)
Jiong Tang (jiong.tang@uconn.edu)

materials involves a suite of inter-related processes, including impregnation of fiber through resin injection and resin curing under an elevated temperature. Because of the complex nature of composite manufacturing, uncertainties inevitably exist in a variety of forms (Mesogitis et al, 2014). The major sources of uncertainties are associated with the material- and process-induced variabilities. These uncertainties will propagate through the entire manufacturing process, and may severely compromise the performance of the final products. Therefore, characterizing the effect of uncertainties becomes an important subject, which as a result can provide guidance for process control and optimization. Composite manufacturing processes are generally analyzed through either experiments or numerical methods such as finite element simulation. Over the years, a series of finite element-based analyses have been conducted that feature multi-physics coupling at multiple temporal and spatial scales (Ersoy et al, 2010; Tavakol et al, 2013; Ding et al, 2015). Recently, Chen and Zhang (2018) developed a multiscale processing model to predict residual stresses buildup in a thermoset composite during the curing process. Their approach involves a macroscale model at the lamina level and a micromechanics model at the fiber and matrix scale. At the macroscale, the composite was modeled as discrete layers of homogeneous transversely isotropic laminae, upon which the effective lamina curing responses will be computed through an Extended Concentric Cylinder Assemblage (ECCA) model at subscale. This approach is efficient in predicting the residual stress distribution in a composite which has been validated experimentally. While significant progresses have been made in deterministic analysis of the nominal process, uncertainty propagation analysis remains to be very challenging. Applying direct Monte Carlo simulation to finite element analysis of manufacturing process generally leads to insurmountable computational cost.

In order to conduct computationally tractable uncertainty analysis, efficient sampling techniques, such as importance sampling (Schueller, 2009; Medina and Taflanidis, 2014), subset simulation (Au and Beck, 2003), and Latin hypercube sampling (Shields and Zhang, 2016) have been attempted. They aim at reducing the sample size, and have shown success in some applications. Nevertheless, such kind of reduction of sample size is still inadequate for finite element based composite manufacturing process simulation which involves complicated multiscale analysis and very costly computational effort even for a single run. In recent years, a new class of methods for uncertainty analysis built upon statistical inference has been suggested. Central to these methods is the development of meta-models or surrogate models to facilitate direct emulation of the input-output relation in manufacturing process. For example, Balokas et al (2018) proposed a neural network to facilitate the quantification of effective elastic property variation of braided composites. Specifically for uncertainty analysis of composites, polynomial chaos expansion (PCE) has attracted some attentions. It essentially is a parametrized method, yielding a spectral representation for the random process in terms of an orthogonal basis (Soize, 2010; Dai et al, 2019). Chen and Qiu (2018) developed a PCE analysis that can accommodate both the random and interval uncertainties. Mehrez et al

(2018) proposed a PCE-based framework to efficiently construct the stochastic models of non-crimp fabric composites in the presence of uncertainties. Peng et al (2019) conducted the uncertainty analysis of a composite laminated plate by using the PCE in combination with the uncertainty type identification criteria. One major challenge in composite uncertainty analysis is that the simulation is intrinsically multiscale with many intermediate variables and final output variables. To tackle the multi-response challenge, the support vector machine (SVM) that is traditionally applied onto single-response regression has been wrapped as a cluster to serve the purpose of multi-response regression (Zhang et al, 2019). Nevertheless, currently the capability of elucidating the correlation of various intermediate variables and final output variables in process simulation is still lacking.

In computational intelligence, Gaussian process (GP) meta-models have shown promising aspects to emulate complex simulations. The basic idea behind Gaussian processes is to extend the discrete multivariate Gaussian distribution on a finite-dimensional space to a random continuous function defined on an infinite-dimensional space (Rasmussen, 2006). It is a non-parametric approach and can be trained with limited number of input-output relations. Moreover, the multi-response Gaussian process (MRGP), an extended variant of the standard single-response Gaussian process, can not only enable multi-response regression, but also capture the intrinsic output correlations in a probabilistic manner (Ghanem et al, 2017). As such, MRGP has been recently employed in a variety of uncertainty quantification analyses (Bostanabad et al, 2018; Du and Padgett, 2020; Zhou and Tang, 2021a). It is worth noting that, although in theory a single MRGP can be used to characterize the variations at multiple scales in the presence of uncertainties, there are implementation challenges. When a large number of variables are to be analyzed, numerical instability may occur in MRGP training, due to the matrix inversion required to optimize the hyperparameters (Arendt et al, 2012a; Zhou and Tang, 2021a). Additionally, in a multiscale model with a large number of intermediate variables and final output variables, the size of training data necessary may become large. This leads to high computational cost in training data acquisition, and very likely will lead to high training cost because the computational complexity of training is at the cubic order of data size (Liu et al, 2018). Fundamentally, in composite manufacturing process, uncertainties are introduced sequentially through different operational variabilities. In other words, the uncertainties take effect with temporal sequence. A single MRGP meta-model cannot account for such effect and thus cannot truly address the uncertainty propagation in composite manufacturing.

In order to tackle the aforementioned challenges and enable the uncertainty propagation analysis, this study proposes a hierarchical computational framework consisting of multiple MRGP meta-models to characterize the multiscale nature of composite manufacturing simulation. This hierarchical structure allows the sequential arrangement of uncertainty analysis throughout the manufacturing process, and can be directly integrated with global sensitivity analysis to quantify the importance of uncertainty propagation

paths. The global sensitivity matrices will be calculated to connect the physical properties at different scales of simulation. Here we employ the Sobol index, which is built upon multivariate statistical analysis (Marrel et al, 2009), to quantify the sensitivities of input-output relations as well as the interactions of various parameters. This framework is flexible, and can be implemented with both numerical and experimental data. The outcome can provide a step-to-step guidance for process optimization and control. The rest of the paper is organized as follows. In Section 2, we first outline a multi-scale finite element simulation model to characterize the underlying behavior of composite manufacturing process, and then present the mathematical formulation of MRGP meta-modeling. In Section 3, a hierarchical computational framework comprised of MRGP meta-modeling and Sobel index-based global sensitivity evaluation is outlined, followed by systematic case studies that illustrate the efficient uncertainty propagation analysis. Section 4 summarizes the current research.

2. Physics based multi-scale modeling for composite manufacturing process and meta-model formulation

In this section, the physics based multi-scale processing model synthesized in a finite element (FE) setting is outlined first. This FE model will be employed to generate training data necessary for the subsequent uncertainty analysis. A hierarchical computational framework based upon the multiple MRGP meta-models and Sobol index is then formulated, which facilitates the uncertainty analysis of composite process simulation.

2.1. Multi-scale finite element simulation for resin curing process

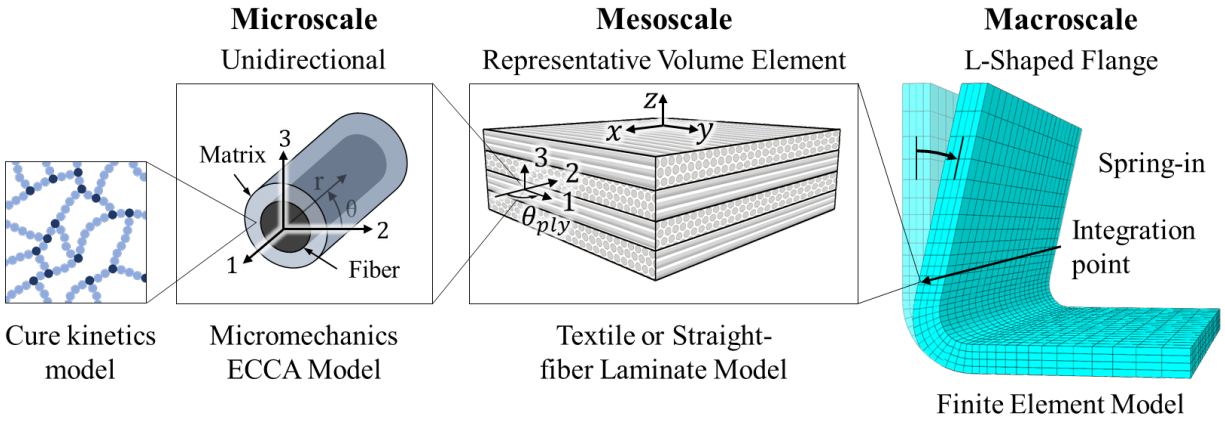

Figure 1. Illustration of multi-scale FE model.

To characterize the influence of the resin curing response on the resulting residual stress buildup in the composite, in this research a multi-scale finite element (FE) model is established, which generally consists of different models that depict the physical features at different hierarchical scales, i.e., microscale,

mesoscale and macroscale of the composite as shown in Figure 1. In this multi-scale FE model, the interface that can exchange the information between different scales is well-constructed. At the macroscale, the composite part is homogenized as an orthotropic solid. At the mesoscale, a Representative Volume Element (RVE) of stacked unidirectional laminae is used to compute the effective composite constitutive relation at each integration of homogenized solid at the macroscale. At the microscale, a micromechanics model is adopted to evaluate the constitutive relation of each unidirectional laminae in the RVE at the mesoscale. Through such multi-scale approach, the physical properties of the entire curing process can be predicted.

As the elevated temperature is usually applied on the laminate to accelerate the cross-linking reaction in the curing process, the heat transfer analysis is implemented first to determine the temperature distribution inside the composite and Degree of Cure (DOC) ϕ based upon the cure kinetics model governed by the equation below (Hubert et al, 2001),

$$\frac{d\phi}{dt} = \left(A_1 \exp\left(-\frac{\Delta E_1}{RT} \right) + A_2 \exp\left(-\frac{\Delta E_2}{RT} \right) \phi^m \right) (1-\phi)^n \tag{1}$$

where R is the universal gas constant. Among the cure kinetics parameters, which can be experimentally characterized, are the frequency factors, A_1 and A_2, activation energies, ΔE_1 and ΔE_2, and the fitting parameters, *m* and *n.* The curing temperature history can be expressed in terms of curing rate solved from Equation (1),

$$\rho_c C_{p,c} \frac{\partial T}{\partial t} = \sum_{n=1}^{3} \frac{\partial}{\partial x_n} \left(k_{n,c} \frac{\partial T}{\partial x_n} \right) + \rho_m \left(1 - V_f \right) H_r \frac{d\phi}{dt} \tag{2}$$

where ρ_c is the effective composite density, $C_{p,c}$ is the effective specific heat, $k_{n,c}$ is the thermal conductivity along the *n*-th direction, ρ_m is the resin density, V_f is the fiber volume fraction, and H_r is the reaction heat. By assuming that the viscoelastic resin behavior is fully relaxed in the rubbery state, and unrelaxed in the glassy state, the resulting stress can be determined as,

$$\sigma(t) = \int_0^t C_i \frac{\partial}{\partial t} \left(\varepsilon - \varepsilon^{\text{th}} - \varepsilon^{\text{ch}} \right) dt \tag{3}$$

where σ is the stress tensor, C_i is the composite stiffness tensor, and $i = R \text{ and } G$ represent the rubbery and glassy states, which correspond to the fully relaxed and unrelaxed stiffness tensors, respectively. ε, ε^{th}, and ε^{ch} are the total, thermal, and chemical strains, respectively. As indicated in Equations (2) and (3), the interested composite properties to be assessed are intrinsically related to the fiber and resin properties.

For composites, even a small sized structure with simple microstructures usually contains a very large number of fibers. It is computationally demanding if a full-scale discrete model is constructed to evaluate the composite properties. To address the computational issue, we establish a multi-scale finite element

modeling approach to characterize the outcome of curing process. The models at different scales created using this approach can effectively capture the structural feature relations through their interfaces. We start from homogenizing the composite as an orthotropic solid at the macroscale in the FE model. The effective properties of the homogenized model can be calculated from the fiber and resin properties using the micromechanics model (Zhang and Wass, 2014; Chen and Zhang, 2018). The goal of the micromechanics model is to determine the effective lamina thermo-chemo-mechanical properties based on the constituent fiber and resin properties. In this study, an efficient analytical method established upon the Extended Concentric Cylinder Assemblage (ECCA) micromechanics models is employed to compute the effective lamina properties. The details of ECCA models have been reported in literature (Chen and Zhang, 2018). The thermo-chemo-mechanical properties of interest, such as the incremental thermal and chemical strains of lamina, can be described as

$$\Delta\varepsilon_{UD}^{\text{th}} = \begin{bmatrix} \alpha_{1,UD} & \alpha_{2,UD} & \alpha_{2,UD} & 0 & 0 & 0 \end{bmatrix}^T \Delta T \tag{4a}$$

$$\Delta\varepsilon_{UD}^{\text{ch}} = \begin{bmatrix} \beta_{1,UD} & \beta_{2,UD} & \beta_{2,UD} & 0 & 0 & 0 \end{bmatrix}^T \Delta\phi \tag{4b}$$

where ΔT is the temperature increment, and $\alpha_{1,UD}$ and $\alpha_{2,UD}$ denote the axial and transverse thermal expansion coefficients of the lamina, respectively. $\Delta\phi$ is the curing increment, and $\beta_{1,UD}$ and $\beta_{2,UD}$ denote the axial and transverse chemical shrinkage coefficients of the lamina, respectively.

The unidirectional properties characterized through the micromechanics models are transferred to the mesoscale model i.e., Repeated Unit Cell (RUC), to determine the effective laminate RUC thermo-chemo-mechanical properties based on the lamina properties. For the laminate composite, the unidirectional properties are represented using the RVE coordinates based on the orientation of each ply. The stacked plies then are homogenized by an extended classical laminated plate theory (CLPT)-based approach (Daniel and Ishai, 2006) to obtain the full 3D properties. For cases requiring accurate bending stiffness of the laminate, it is recommended to model each ply explicitly in the macroscale FE model with definition of the corresponding material orientations. In this study, the mesoscale model represents a plain weave textile ply as a crossply laminate, which is built as several stacked layers together to reduce the computational cost. Following this approach, the associated thermo-chemo-mechanical properties of the laminate RVE can eventually be derived. Then, the incremental thermal and chemical strains $\Delta\varepsilon^{\text{th}}$ and $\Delta\varepsilon^{\text{ch}}$ in a symmetrical laminate RVE can be described as,

$$\Delta\varepsilon^{\text{th}} = \begin{bmatrix} \alpha_x & \alpha_y & \alpha_z & 0 & 0 & 0 \end{bmatrix}^T \Delta T \tag{5a}$$

$$\Delta\varepsilon^{\text{ch}} = \begin{bmatrix} \beta_x & \beta_y & \beta_z & 0 & 0 & 0 \end{bmatrix}^T \Delta\phi \tag{5b}$$

where α_x, α_y, and α_z denote the thermal expansion coefficients of the laminate, and β_x, β_y, and β_z denote the chemical shrinkage coefficients of the laminate. The stress increment is updated according to Equation (3), and the effective laminate properties are passed from the mesoscale to the macroscale through the Jacobian matrix to the FE solver.

2.2. Probabilistic representation of uncertainty sources

The property relations in multi-scale simulation outlined in Section 2.1 are depicted in Figure 2. The variables in the leftmost column represent the mechanical and thermal properties of the raw material. The variables in the middle two columns represent the properties of composites at the microscale and mesoscale, respectively. The single structural property of interest at the macroscale is the spring-in angle as indicated in the rightmost column. The physical meaning of those variables can be referred to Tables 4 and 5 in the subsequent case illustrations (Section 3). Uncertainties inevitably exist in the composite models at different scales and will propagate through the entire simulation. As a result, the uncertainties will lead to the variability of final composite properties and output variables.

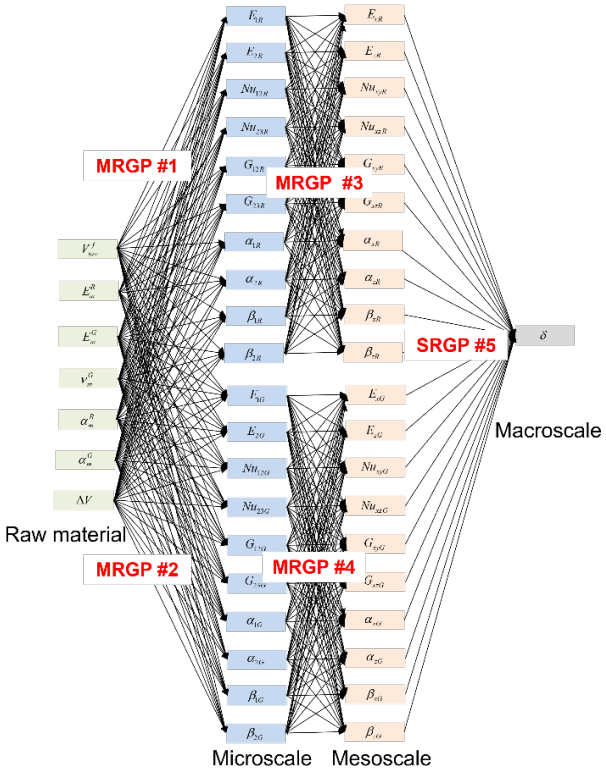

Figure 2. Illustration of property relations in multi-scale FE simulation and hierarchical MRGP meta-models.

Uncertainty analysis generally starts with the characterization of uncertainty sources. Once uncertainty sources are probabilistically defined, Monte Carlo sampling or perturbation-based approximation methods may be applied in conjunction with FE processing model to analyze the uncertainty consequence (Grover et al, 2017). A random field (RF), also known as a stochastic process, is a collection of random variables, which is commonly used to represent the characteristics of uncertainty sources (Gallager, 2013; Khristenko et al, 2020). Let a probability space be denoted as $\{\Omega, F, P\}$ where Ω is the sample space, F is the subset of Ω with probability measure P. Given the probability space $\{\Omega, F, P\}$, a RF of can be described as

$$R(\mathbf{x}, F) = \{F_t : t \in T\} \tag{6}$$

where $\mathbf{x}$ is a vector/collection of uncertainty variables that are random. F_t is the sampled outcome in F. T is a topological space containing the indices of $\mathbf{x}$. The RF of $\mathbf{x}$ can be either continuous or discrete. The discrete representation allows the indices in topological space T to be identified with a discrete set of points, while the continuous representation allows $\mathbf{x}$ to be function valued variables.

As will be described in the subsequent section, we propose a hierarchical computational framework built upon multiple meta-models, shown in Figure 2, to quantify the relations of properties at two adjacent scales. With the further integration of global sensitivity analysis, the uncertainty propagation analysis of the multi-scale simulation can be facilitated. In this framework, the uncertainty sources in the FE processing model mainly include the material properties of resin and fiber, as well as the operational variables. These quantities change spatially or temporally as the manufacturing process proceeds, which can be represented by the RF. Gaussian RF (GRF) is a well-known type of RF, in which the random variables can be explicitly represented by the mean and covariance functions. In this study, we use GRF to model the uncertainties since it tightly aligns with the underlying idea of the Gaussian process to be adopted. It is worth noting that Gaussian process essentially is a GRF when the continuous domain of random variables is considered.

2.3. Hierarchical framework integrated with MRGP meta-modeling and global sensitivity analysis

Uncertainty analysis generally is executed upon the repetitive evaluation based on simulation model over the entire uncertainty space. This can be computationally prohibitive when the simulation model is complex. Hence, in this research the multi-response Gaussian process (MRGP) meta-modeling technique is employed to emulate the FE simulation to accelerate the uncertainty analysis. A series of sequentially arranged MRGP meta-models are configured (Figure 2). This further allows the global sensitivity.

2.3.1 Multi-response Gaussian process (MRGP) for uncertainty quantification (UQ) analysis

GP is a popular meta-modeling approach that has been used in a variety of applications including design optimization (Zhou and Tang, 2017; Li and Wang, 2018), model calibration (Arendt et al, 2012a; Arendt et al, 2012b, Zhou and Tang, 2021b) and uncertainty quantification (Wan et al, 2014; Zhou and Tang, 2018).

MRGP is a special variant of GP where the output is a vector. Given the process input $\mathbf{x}=[x_1,x_2....x_d]^T$ and associated process output $\mathbf{y}=[y_1,y_2....y_r]^T$ at a particular scale, an MRGP can be represented as

$$\mathbf{y} \sim \bullet_r(\mathbf{H}(\mathbf{x})\boldsymbol{\beta}, \mathbf{Q}\otimes k(\mathbf{x},\mathbf{x}')) \tag{7}$$

where $\bullet_r$ denotes a *r*-dimensional MRGP, $\mathbf{H}(\mathbf{x})\boldsymbol{\beta}$ denotes the response mean vector, $\mathbf{Q}$ is the $r\times r$ non-spatial correlation matrix to account for the statistical correlation of responses, and $k(\mathbf{x},\mathbf{x}')$ is the covariance kernel that can be computed upon the spatial distance between $\mathbf{x}$ and $\mathbf{x}'$. $\mathbf{Q}\otimes k(\mathbf{x},\mathbf{x}')$ thus represents the overall covariance of MRGP output ***y***, where $\otimes$ denotes the Kronecker product. Various covariance kernels are available for GP construction (Rasmussen and Williams, 2006). For example, a radial basis function (RBF) covariance kernel is written as

$$k(\mathbf{x}_i,\mathbf{x}_j)=\sigma_f^2 e^{-\frac{(\mathbf{x}_i-\mathbf{x}_j)^T(\mathbf{x}_i-\mathbf{x}_j)}{2l}}+\sigma_n^2\delta_{ij} \tag{8}$$

The covariance kernel is characterized by unknown parameters, i.e., $\vartheta=[\sigma_f^2,l,\sigma_n^2]$. Signal variance σ_f^2 is a scaling factor, representing the variation of function values from their mean. Small values of σ_f^2 indicate functions that stay close to their mean value, and larger values allow more variations. Lengthscale l describes how smooth a function is. σ_n^2 is the noise term that allows to learn the observation noise/uncertainty from data. These parameters collectively control the smoothness of response change across the input space. As will be shown later, the unknowns $\boldsymbol{\beta}$ and $\mathbf{Q}$ are dependent on $\vartheta=[\sigma_f^2,l,\sigma_n^2]$. $\vartheta=[\sigma_f^2,l,\sigma_n^2]$ thus can be referred to as hyperparameters to be optimized through MRGP training. The hyperparameters enable the MRGP to model a wide range of random processes.

In this research, the input-output relations generated via the high-fidelity FE model are used to train MRGP meta-model. Assume we have a set of observed inputs $\mathbf{X}=[\mathbf{x}_1,\mathbf{x}_2,...\mathbf{x}_N]$ and outputs $\mathbf{Y}=[\mathbf{Y}_1,\mathbf{Y}_2,...\mathbf{Y}_N]$, where *N* is the number of observation/training data. The training process follows the scheme of maximum likelihood estimation (MLE) built upon the Bayesian formula (Rasmussen and Williams, 2006) in terms of multivariate Gaussian disctribution given below,

$$p(\mathbf{Y}\mid\mathbf{X},\vartheta)=(2\pi)^{-\frac{r.N}{2}}(\det\mathbf{Q})^{-\frac{N}{2}}(\det\boldsymbol{\Sigma})^{-\frac{r}{2}}\exp\left\{-\frac{1}{2}\mathrm{vec}(\mathbf{Y}-\mathbf{H}(\mathbf{X})\boldsymbol{\beta})^T(\mathbf{Q}\otimes\boldsymbol{\Sigma})^{-1}\mathrm{vec}(\mathbf{Y}-\mathbf{H}(\mathbf{X})\boldsymbol{\beta})\right\} \tag{9}$$

where $\mathrm{vec}(.)$ is the vector operator, converting a 2-dimensional matrix into a vector. $\boldsymbol{\Sigma}$ is a covariance matrix whose entry is $k(\mathbf{x},\mathbf{x}')$ shown in Equation (7). To facilitate the optimization, a natural logarithm is applied to both sides of Equation (9), yielding

$$\ln(p(\mathbf{Y}\mid\mathbf{X},\vartheta))=-\frac{r.N}{2}\ln(2\pi)-\frac{N}{2}\ln(\det\mathbf{Q})-\frac{r}{2}\ln(\det\boldsymbol{\Sigma})-\frac{1}{2}\mathrm{vec}(\mathbf{Y}-\mathbf{H}(\mathbf{X})\boldsymbol{\beta})^T(\mathbf{Q}\otimes\boldsymbol{\Sigma})^{-1}\mathrm{vec}(\mathbf{Y}-\mathbf{H}(\mathbf{X})\boldsymbol{\beta})$$

(10)

The optimal $\hat{\boldsymbol{\beta}}$ can be found by setting the derivative of the above expression with respect to $\boldsymbol{\beta}$ to be zero. $\hat{\boldsymbol{\beta}}$ thus is calculated as a function of hyperparameters $\vartheta = [\sigma_f^2, l, \sigma_n^2]$,

$$\hat{\boldsymbol{\beta}} = [\mathbf{H}(\mathbf{X})^T \boldsymbol{\Sigma}(\vartheta)\mathbf{H}(\mathbf{X})]^{-1}\mathbf{H}(\mathbf{X})^T \boldsymbol{\Sigma}(\vartheta)\mathbf{Y} \tag{11}$$

Similarly, the optimal $\mathbf{Q}$ is derived as

$$\hat{\mathbf{Q}} = \frac{1}{N}(\mathbf{Y} - \mathbf{H}(\mathbf{X})\hat{\boldsymbol{\beta}})^T \boldsymbol{\Sigma}(\vartheta)^{-1}(\mathbf{Y} - \mathbf{H}(\mathbf{X})\hat{\boldsymbol{\beta}}) \tag{12}$$

Substituting Equations (11) and (12) into Equation (10) yields the natural logarithm of likelihood that is only associated with hyperparameters $\vartheta = [\sigma_f^2, l, \sigma_n^2]$. Prior knowledge can be used to adjust the hyperparameters and model a spatially varying quantity. The well-developed optimization techniques also can be employed to rigorously identify the proper hyperparameters. Care should be taken to tackle the numerical issue caused by the matrix operations in MRGP training (Arendt et al, 2012a). Once the MRGP meta-model is trained, the predicted output $\mathbf{Y}^*$ of the target input $\mathbf{X}^*$ based on the posterior of MRGP and optimized $\hat{\vartheta} = [\hat{\sigma}_f^2, \hat{l}, \hat{\sigma}_n^2]$ is described as

$$\mathbf{Y}^* \mid \mathbf{Y}, \mathbf{X}, \mathbf{X}^*, \hat{\vartheta} \sim \bullet_r(\boldsymbol{\mu}, \boldsymbol{\Theta}) \tag{13}$$

where the posterior mean and covariance functions under the optimized hyper-parameters are, respectively,

$$\boldsymbol{\mu} = \mathbf{H}(\mathbf{X}^*)\hat{\boldsymbol{\beta}} + \hat{\boldsymbol{\Sigma}}^{*T}\hat{\boldsymbol{\Sigma}}^{-1}(\mathbf{Y} - \mathbf{H}(\mathbf{X})\hat{\boldsymbol{\beta}}) \qquad \boldsymbol{\Theta} = \hat{\mathbf{Q}} \otimes (\hat{\boldsymbol{\Sigma}}^{**} - \hat{\boldsymbol{\Sigma}}^{*T}\hat{\boldsymbol{\Sigma}}^{-1}\hat{\boldsymbol{\Sigma}}^{*}) \tag{14a,b}$$

where $\hat{\boldsymbol{\Sigma}}^* = \hat{\boldsymbol{\Sigma}}(\mathbf{X}, \mathbf{X}^*)$ and $\hat{\boldsymbol{\Sigma}}^{**} = \hat{\boldsymbol{\Sigma}}(\mathbf{X}^*, \mathbf{X}^*)$.

As indicated in Figure 2, in this research 5 MRGP meta-models are constructed to map the properties at different, adjacent scales. Specifically, MRGP #1 and #2 link the material properties with composite properties in the resin and glassy states respectively at the microscale. MRGP #3 and #4 continuously build the relations between the composite properties at the microscale and mesoscale. Considering that the composite properties in the rubbery state are weakly correlated with that in the glassy state, no MRGP meta-models are needed to identify the interstate property mapping for the simplicity of analysis. The last MRGP essentially is a single-response Gaussian process (SRGP) since its output is a scalar, i.e., spring-in angle, which is influenced collectively by all composite properties at the mesoscale.

2.3.2 Integration of global Sobol sensitivity for uncertainty propagation (UP) analysis

As shown in Figure 2, the relations of the physical variables in the multi-scale simulation exhibit a complex, networked architecture. Each line that connects two physical variables denotes the uncertainty propagation path. To unveil the underlying mechanism of UP, the impact of the antecedent variable with

respect to the consequent variable at each path needs to be quantitatively assessed. This can be realized by integrating the global sensitivity analysis, in which the sensitivity item is used as an impact measure. The global sensitivity matrices at different scales can be efficiently calculated based upon the MRGP meta-models. As a result, the entire UP network will be constructed. Sobol index, as a particular form of global sensitivity, is adopted in this research.

Sobol index is built upon the probabilistic framework, where the key idea is to decompose the output variance into fractions which can be attributed to inputs or sets of inputs (Sobol and Kucherenko, 2009). In other words, Sobol index intends to determine how much of the variability in the model output is dependent upon each of the inputs or upon an interaction between different inputs. This leads to the multivariate statistical analysis. Besides, it can deal with nonlinear input-output relations (Homma and Saltelli, 1996), which commonly exist in manufacturing processes. In this approach, we let the input vector be denoted as $\mathbf{x} = [x_1, x_2 ... x_d]^T$ where the variables are mutually independent, and let the scalar output be denoted as $y = f(\mathbf{x})$ upon the target model $f(.)$. The functional decomposition of variables referred to as functional ANOVA (Efron and Stein, 1981) can be expressed as

$$Var(y) = \sum_{i}^{d} D_i(y) + \sum_{i<j}^{d} D_{ij}(y) + ... + D_{1,2...d}(y) \tag{15}$$

where $D_i(y) = Var[E(y \mid x_i)]$, $D_{ij}(y) = Var[E(y \mid x_i, x_j)] - D_i(y) - D_j(y)$ and so on for higher order interactions. Sobol indices or variance-based sensitivity indices can be obtained as

$$S_i = \frac{D_i(y)}{Var(y)}, \qquad S_{ij} = \frac{D_{ij}(y)}{Var(y)}, \qquad \cdots \tag{16}$$

Based on Equations (15) and (16), we have that the sum of all Sobol indices is 1, i.e.,

$$\sum_{i}^{d} S_i + \sum_{i<j}^{d} S_{ij} + ... + S_{1,2...d} = 1 \tag{17}$$

The number of Sobol indices, i.e., $2^d - 1$, grows exponentially with respect to the dimension of inputs *d*. The Sobol indices can be estimated through Monte Carlo sampling-based analysis. A large number of samples usually are required to calculate each Sobol index (Saltelli, 2002). For the sake of computational convenience, it is suggested to only account for the main effects using the lower-order Sobol indices (Ioose and Lemaitre, 2015). These lower-order Sobol indices can provide sufficient information on the global model sensitivities. It is worth mentioning that Sobol indices are originally formulated upon the target model with single output/scalar. To characterize the lower-order Sobol indices of inputs on multiple outputs, a loop computation is required to establish a sensitivity matrix, which characterizes the variable correlations. The entire UP network consisting of multiple sensitivity matrices is constructed and shown schematically in Figure 3.

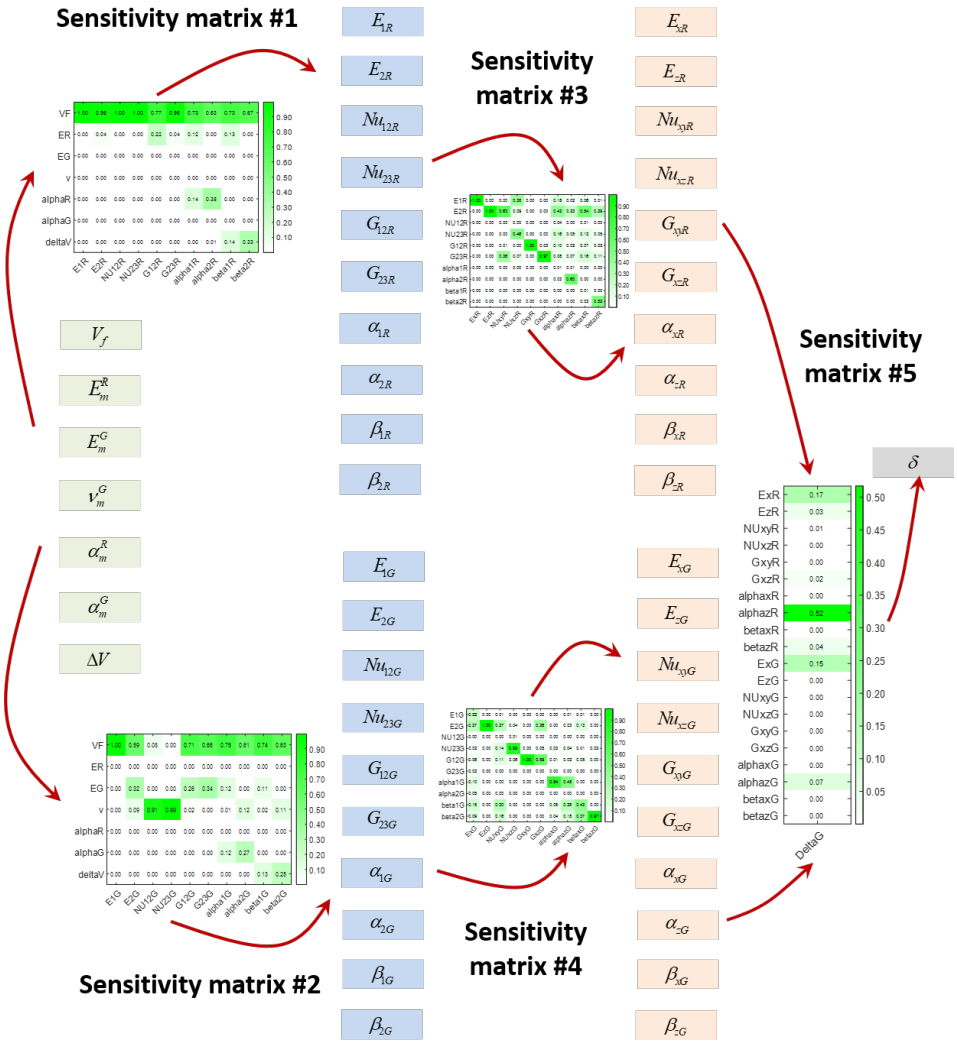

Figure 3. Illustration of UP (uncertainty propagation) network consisting of global sensivity matrices.

3. Case studies and illustrations

In this section, we carry out systematic case studies to demonstrate the capability of this new framework. A deterministic multi-scale FE model is built to simulate the composite curing process on a curved composite beam. Given the material variability of fiber and resin used, the framework employing MRGP and global sensitivity analysis is then implemented for the uncertainty analysis.

3.1. Multi-scale FE simulation

3.1.1. Simulation of spring-in angle using composite processing FE model

We start from the FE model, which will be used to provide training data for MRGP emulation. For model validation purpose, the fiber and resin properties used in the model match with an associated experimental investigation. Specifically, carbon fiber is utilized in the experiment and its thermo-

mechanical properties are given in Table 1 assuming that the fiber is an elastic, transversely isotropic solid. Additionally, EPON 862/W resin system is used, whose thermo-chemo-mechanical properties and parameters to build the cure kinetics FE model are given respectively in Tables 2 and 3.

Table 1. Thermo-mechanical properties of the carbon fibers used (Heinrich et al, 2013)

Symbol	Definition	Value
ρ_f	Density	1800 kg/m^3
$C_{P,f}$	Specific heat	1130 J/kg/K
$k_{1,f}$	Axial conductivity	6.83 W/m/K
$E_{1,f}$	Axial modulus	231E+09 Pa
$E_{2,f}$	Transverse modulus	15E+09 Pa
$\nu_{12,f}$	Axial Poisson's ratio	0.27
$G_{12,f}$	Axial shear modulus	2.40E+04 Pa
$G_{23,f}$	Transverse shear modulus	5.01E+03 Pa
$\alpha_{1,f}$	Axial CTE	-9.00E-07 K^{-1}
$\alpha_{2,f}$	Transverse CTE	7.20E-06 K^{-1}

Table 2. Thermo-chemo-mechanical properties of EPON 862/W

Symbol	Definition	Value
ρ_m	Density	1200 kg/m^3
$C_{P,m}$	Specific heat	1150 J/kg/K
k_m	Thermal conductivity	0.188 W/m/K
T_g^0	Glass transition temperature of uncured resin	246 K
T_g^∞	Glass transition temperature of fully-cured resin	383 K
α_m^R	CTE in the rubbery state	1.82E-04 K^{-1}
α_m^G	CTE in the glassy state	7.78E-05 K^{-1}
ΔV	Chemical shrinkage (volume)	-3.72E-02
E_m^R	Modulus at the glassy state	3.24E+07 Pa
E_m^G	Modulus at the glassy state	3.24E+09 Pa
ν_m^G	Poisson's ratio at the glassy state	0.35
λ	Fitting parameter	0.392
ϕ_{gel}	DOC at gelation	0.71

Table 3. Parameters used in the cure kinetics model for EPON 862/W (Heinrich et al, 2013)

Cure kinetics parameter	Characterized value	Value from literature
A_1	0 s^{-1}	0 s^{-1}
ΔE_1	-	-
A_2	7098 s^{-1}	6488 s^{-1}
ΔE_2	5.5E+04 J/mol	5.3E+04 J/mol
m	0.40	0.39
n	1.65	1.67
H_r	406.12 J/g	399.00 J/g

Following the multi-scale modeling approach outlined in Section 2.1, the FE model is constructed using the commercial software ABAQUS 2017 (Figure 4a). In the FE model, 3D quadratic solid elements C3D20 is adopted to model the curved composite beam that is approximately treated as a homogeneous anisotropic material. The cure- and temperature- dependent parameters are computed using the model introduced in Section 2.1, which are implemented as a user-defined subroutine. The cure cycle is pre-specified as a temperature profile, starting at room temperature of 25°C, ramping to the cure temperature of 170°C in 15 min., and holding the cure temperature for 120 min. before cooling back to room temperature in 45 min. Such cure cycle is applied to the surface of the composite beam to conduct the FE-based heat transfer analysis. Using the input parameters defined in Tables 1-3, the spring-in angle can be calculated via measuring the slope of the flange. The final spring-in angle in this case is predicted as 2.1° via FE analysis.

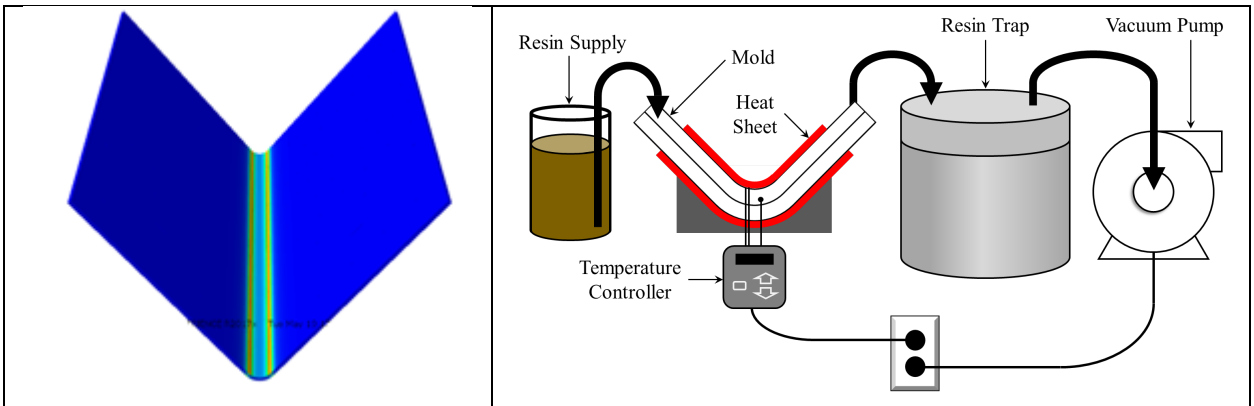

Figure 4. L-shape composite flange analysis (a) FE modeling; (b) Laboratory setup.

3.1.2. Fabrication of L-shaped flanges for experimental investigation

To validate the effectiveness of the multi-scale FE modeling, a curved composite beam was fabricated using 16 plies of plain weave carbon-fiber fabric via the resin transfer molding (RTM) technique (Figure 4b). The adhesive was sprayed onto the open RTM L-shaped model, and dissolves during the resin infusion process. To facilitate the demolding procedure at the end of the curing and improve the surface quality of the finished composite part, peel-ply was draped into the mold, which was held in place by the adhesive. Such draping procedure was repeated for all 16 layers of fabric, followed by another peel-ply on the top of the layup to contact the top mold. The top and bottom molds were combined through the bolted joint. A proper torque then was properly applied, and tubes were used to connect the inlet and outlet ports. The temperature of the mold was regulated by the temperature controller set using a heat sheet affixed to the surface. The inlet tube was clamped shut and the outlet tube was connected to a resin trap, which prevents the excessive resin to destroy the vacuum pump. The vacuum pump was powered to remove the air from the system. The inlet tube was placed into the resin and unclamped, which allows the resin to flow into the mold and infuse the fiber layup.

Following the resin infusion process, the composite flange was cured at 170°C for 120 min. The process-dependent parameters involved in this experiment are kept identical to the ones used in the multi-scale FE simulation. The demolding procedure was carried out to obtain the cured composite part after the curing process. Subsequently, the spring-in angle of the curved composite beam was measured using an electronic protractor, with an average value of 1.9° (Chen, 2019). Since in this research the experimental result is used for qualitative assessment of the physics-based model, it agrees with the numerical prediction (i.e., 2.1°) reasonably well. From algorithmic perspective, the proposed MRGP allows one to account for the data error/uncertainty by incorporating the noise term, i.e., σ_n^2 into the covariance kernel (Equation (8)). Furthermore, MRGP fundamentally is a probabilistic meta-model that is trained through the Bayesian optimization. As such, its prediction can take the data error/uncertainty into consideration. For these reasons, we believe that the current FE model is adequate for subsequent uncertainty analysis.

3.2. Establishment of hierarchical MRGP meta-models for efficient UQ

Various uncertainty sources that span across the multi-scale simulation inevitably exist, which yields the variations of interested physical properties at different temporal and spatial scales. For illustration, 7 uncertainty variables representing the resin properties of raw material are taken into account since they are more prone to manufacturing variability. GRF is used to model such uncertainties in the form of multivariate Gaussian distribution. The uncertainty variables and their statistical moments of distributions are given in Table 4. The multi-scale simulation is schematically depicted in Figure 2. There are 10 interested physical properties at the microscale and mesoscale respectively, and only spring-in angle of interest at the macroscale. The details of these interested physical properties are given in Table 5. The

values of total 41 properties are calculated using ABAQUS using sampled uncertainty variables. Statistical sampling, i.e., the Latin hypercube approach (Helton and Davis, 2003) is employed to generate uncertainty samples over entire uncertainty space. These samples are then substituted into the deterministic FE model to produce the interested property values. Following this procedure, 1,000 benchmark input-output relations are generated. The entire dataset will then be used to train and validate the MRGP meta-models.

Table 4. Uncertainty sources characterized with GRF

Symbol/Notation	Definition	Mean	Standard Deviation
V_f (VF)	Fiber volume fraction	0.58	0.0106
$E_R^{(m)}$ (ER)	Young's modulus of resin in the rubbery state (Pa)	3.24E+07	6.28E+05
$E_G^{(m)}$ (EG)	Young's modulus of resin in the glassy state (Pa)	3.24E+09	6.28E+07
$\nu^{(m)}$ (v)	Poisson ratio of resin in the glassy state	0.35	0.007
$\alpha_R^{(m)}$ (alphaR)	CTE of resin in the rubbery state (K^{-1})	1.82E-04	3.64E-06
$\alpha_G^{(m)}$ (alphaG)	CTE of resin in the glassy state (K^{-1})	7.78E-05	1.556E-06
ΔV (deltaV)	Chemical shrinkage	-0.0372	0.000744

Table 5. Physical properties obtained from FE simulation

	Rubbery State Variable	Glassy State Variable	Definition
Microscale (Unidirectional)	E_{1R} (E1R)	E_{1G} (E1G)	Young's moduli
	E_{2R} (E2R)	E_{2G} (E2G)	
	Nu_{1R} (NU12R)	Nu_{1G} (NU12G)	Poisson's ratio
	Nu_{2R} (NU23R)	Nu_{2G} (NU23G)	
	G_{12R} (G12R)	G_{12G} (G12G)	Shear moduli
	G_{23R} (G23R)	G_{23G} (G23G)	
	α_{1R} (alpha1R)	α_{1G} (alpha1G)	Coefficient of thermal expansion (CTE)
	α_{2R} (alpha2R)	α_{2G} (alpha2G)	
	β_{1R} (beta1R)	β_{1G} (beta1G)	Coefficient of chemical shrinkage
	β_{2R} (beta2R)	β_{2G} (beta2G)	
Mesoscale (Laminate)	E_{xR} (ExR)	E_{xG} (ExG)	Young's moduli
	E_{zR} (EzR)	E_{zG} (EzG)	
	Nu_{xyR} (NUxyR)	Nu_{xyG} (NUxyG)	Poisson's ratio
	Nu_{xzR} (NUxzR)	Nu_{xzG} (NUxzG)	
	G_{xyR} (GxyR)	G_{xyG} (GxyG)	Shear moduli
	G_{xzR} (GxzR)	G_{xzG} (GxzG)	

	α_{xR} (alphaxR)	α_{xG} (alphaxG)	Coefficient of thermal expansion (CTE)
	α_{zR} (alphazR)	α_{zG} (alphazG)	
	β_{xR} (betaxR)	β_{xG} (betaxG)	Coefficient of chemical shrinkage
	β_{zR} (betazR)	β_{zG} (betazG)	
Macroscale (Structural)	Final spring-in angle δ		

Note, subscript *1*, *2*, *3* and *x*, *y*, *z* denote the axes in local coordinate systems at different scales. Subscript *R* and *G* denote the rubbery and glassy states, respectively.

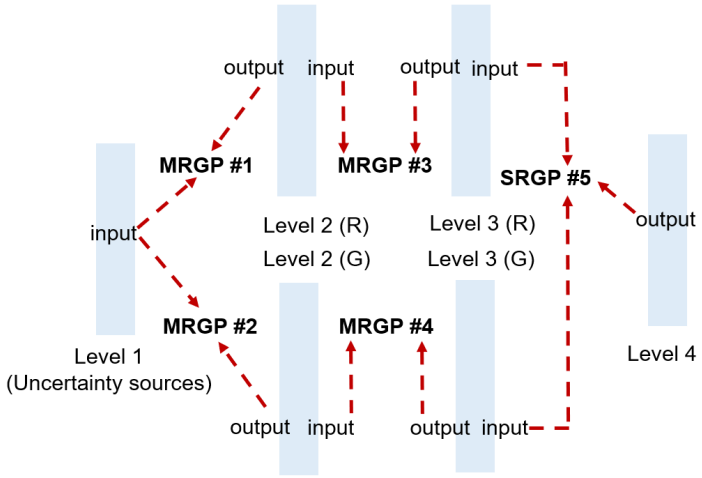

(a)

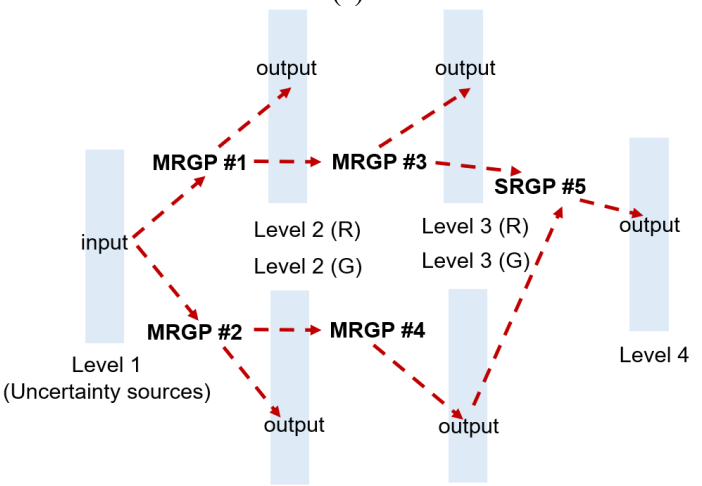

(b)

Figure 5. MRGP meta-model emulation. (a) Training scheme; (b) Testing scheme.

An important step in UQ analysis is to establish the MRGP meta-models. As mentioned, 5 MRGP meta-models are employed to emulate the multi-scale processing simulation in this research (Figure 2). The mean and covariance functions of each MRGP meta-model are determined using trial-and-error-based grid search strategy (Dangeti, 2017). The details of mean and covariance functions selected are listed in Table 6. 200

out of 1,000 data points are randomly selected for training, and the rest of data points are used for testing/validation. The normal training scheme is adopted for all meta-models (Figure 5a). However, a different testing scheme i.e., sequential testing, is utilized, in which only uncertainties at raw material level are considered as inputs (Figure 5b). The inputs of MRGP #2 are the predicted outputs of MRGP #1, and so on. This new testing scheme takes the propagation of prediction error into account, which requires the highly reliable MRGP meta-models in order to ensure the excellent accuracy of final spring-in angle prediction. The regression accuracy metrics used include the mean absolute percentage error (MAPE) and coefficient of determination calculated upon the testing and predicted outputs, respectively given as

$$\hat{\varepsilon} = \sum_{i=}^{M} \left| \frac{y_i^{(p)} - y_i^{(t)}}{y_i^{(t)}} \right| / M \times 100\,(\%) \tag{18a}$$

$$R^2 = \frac{(\sum_{i=1}^{M}((y_i^{(p)} - E(\mathbf{y}^{(p)}))(y_i^{(t)} - E(\mathbf{y}^{(t)})))^2}{(\sum_{i=1}^{M}(y_i^{(p)} - E(\mathbf{y}^{(p)})^2)(\sum_{i=1}^{M}(y_i^{(t)} - E(\mathbf{y}^{(t)})^2)} \tag{18b}$$

where M is the number of testing samples, i.e., 800 in this case. Superscripts p and t indicate the predicted and actual values, respectively. We also let $\hat{\varepsilon} \in [0\ 100]$ and $R^2 \in [0\ 1]$. The coefficient of determination is a statistical measurement that examines how differences in one variable can be explained by the difference in a second variable, when predicting the outcome of a given event. This metric, also known as R-squared (R^2), can assess how strong the linear relationship is between two variables (Draper and Smith, 1998). Larger value of R^2 indicates higher accuracy.

Table 6. Kernel/functions adopted in MRGP meta-modeling

	Mean function		Covariance function	
MRGP #1, #2, #3, #4	Linear mean	$\boldsymbol{\mu} = \mathbf{H}(\mathbf{x})\boldsymbol{\beta}$	Isotropic Radial basis function (RBF)	$k(\mathbf{x}_i, \mathbf{x}_j) = \sigma_f^2 e^{-\frac{(\mathbf{x}_i - \mathbf{x}_j)^T(\mathbf{x}_i - \mathbf{x}_j)}{2l}} + \sigma_n^2 \delta_{ij}$
MRGP #5	Zero mean	$\mathbf{0}$	Rational Quadratic (RQ)	$k(\mathbf{x}_i, \mathbf{x}_j) = b^2 (1 + \frac{(\mathbf{x}_i - \mathbf{x}_j)^T(\mathbf{x}_i - \mathbf{x}_j)}{2\alpha l^2})^{-\alpha} + \sigma_n^2 \delta_{ij}$

We adopt the repeated random subsampling cross validation (Refaeilzadeh et al, 1998) to systematically investigate the meta-mode performance using the abovementioned metrics. The results are shown in Figures 6 and 7. It is noticed that the prediction accuracy of all variables using both metrics is very good except for the MAPE level for variable "alpha1G" (Figure 6b), which is around 5-10% under different emulation runs. We further examine the root cause of such error level by plotting both the actual and predicted values of

the variable “alpha1G” in Figure 8. It is found that the actual values of this variable have quite small magnitude order. Specifically, some actual values are very close to zeros, which results in large MAPE level even though the discrepancies are very small. For example, the actual value of highlighted data point in Figure 8 is 7.12×10^{-11}. While its prediction appears to be consistent with the actual value, an MAPE around 127% is yielded. The results celarly show the excellent acuracy and robustness of the MRGP meta-models. The well-established MRGP meta-models can then be used to facilitate the efficient UQ analysis, yielding the statistical distribution of interested physical properties at different scales. The comparison between the actual and predicted distributions are shown in Figures 9-11. Overall, the agreement of the distributions provides the consistent observation of the good performance of MRGP meta-models.

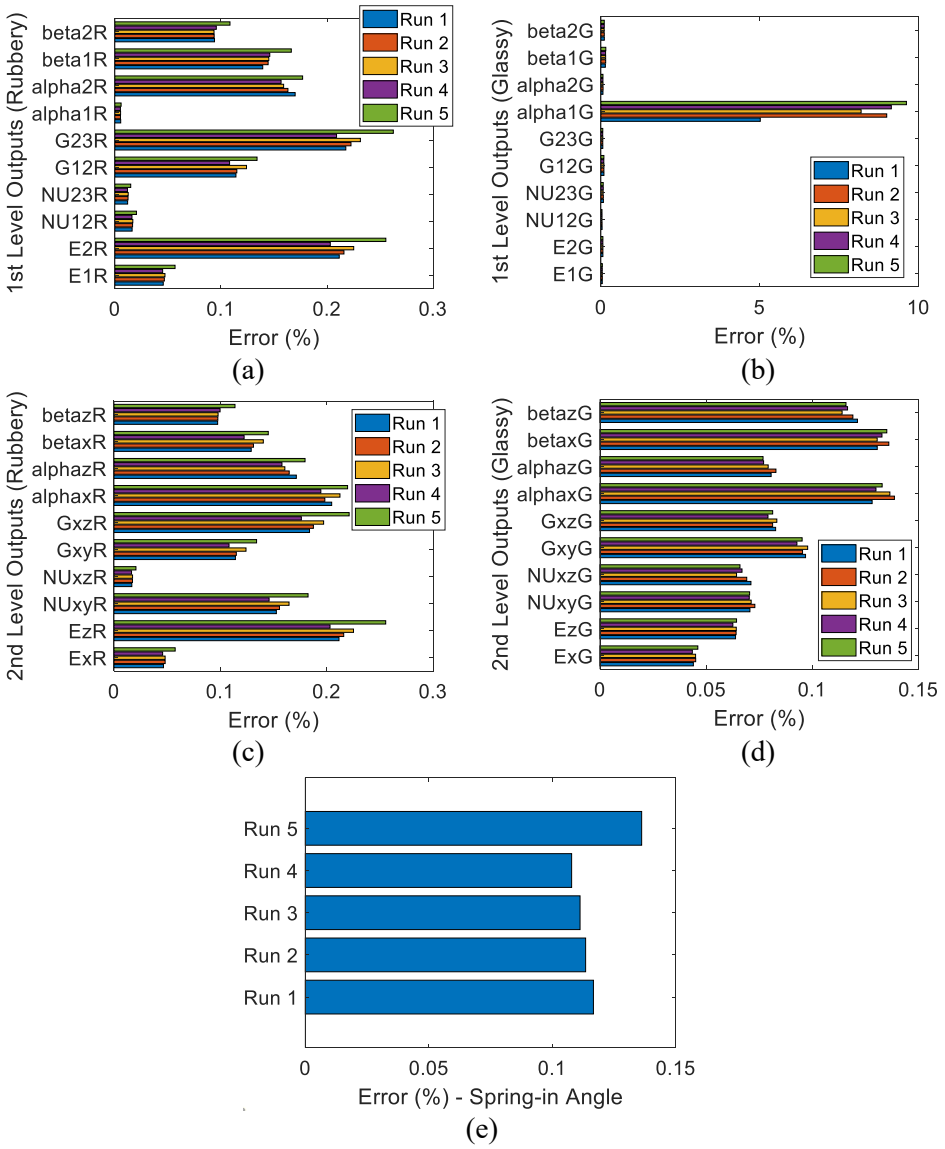

Figure 6. Cross validation result of MRGP meta-models (MAPE) (a) MRGP #1; (b) MRGP #2; (c) MRGP #3; (d) MRGP #4; (e) MRGP #5.

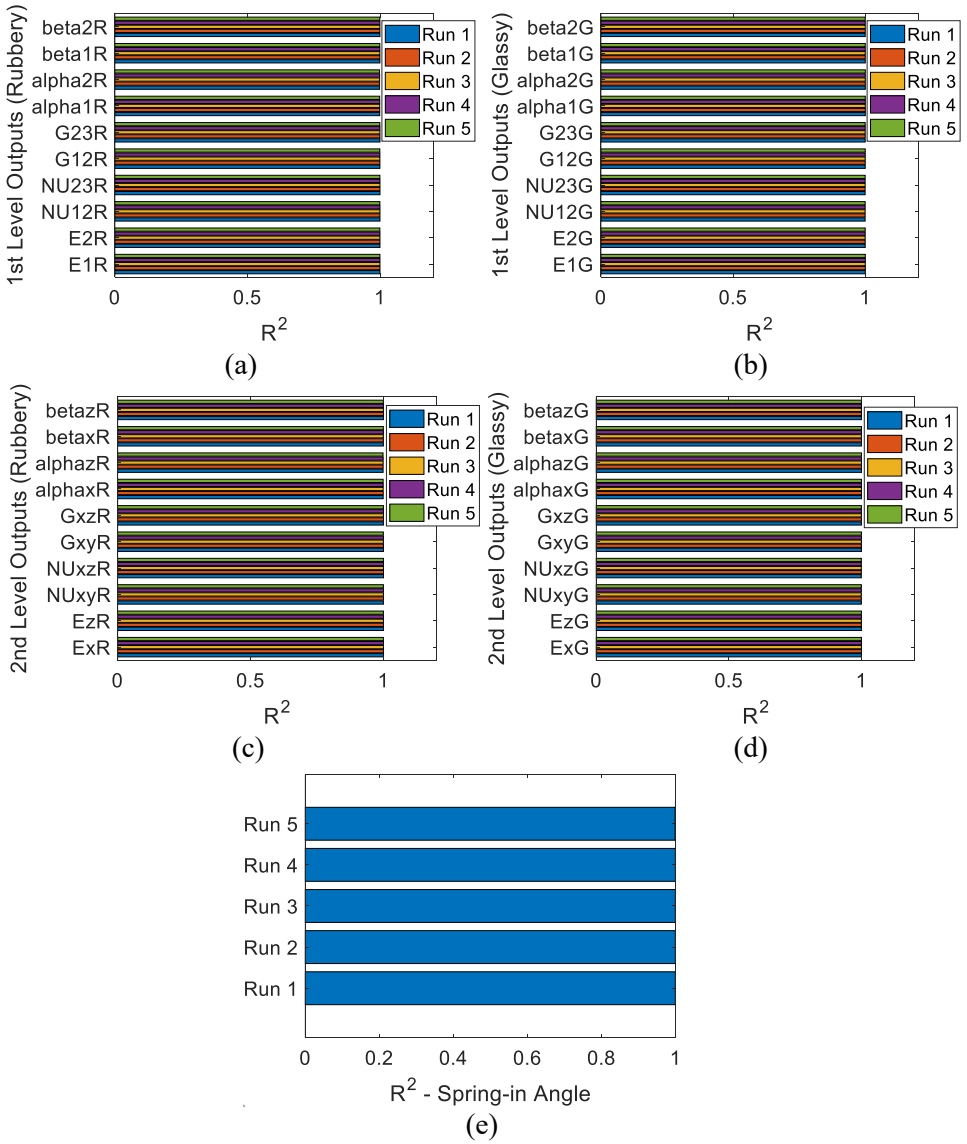

Figure 7. Cross validation result of MRGP meta-models (coefficient of determination). (a) MRGP #1; (b) MRGP #2; (c) MRGP #3; (d) MRGP #4; (e) MRGP #5.

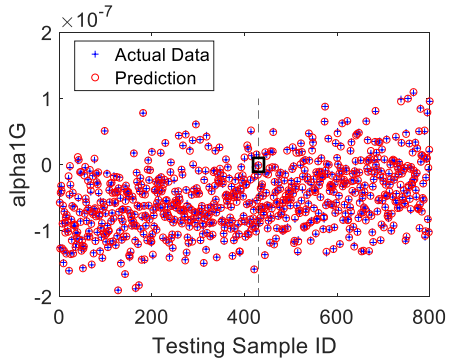

Figure 8. Comparison between actual and predicted values of the variable “alpha1G”.

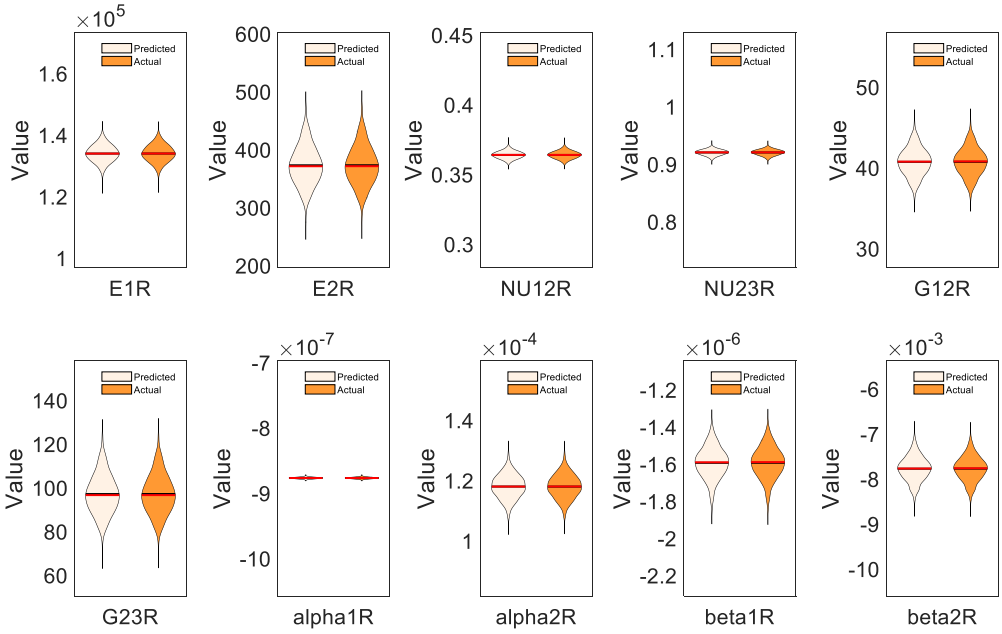

(a)

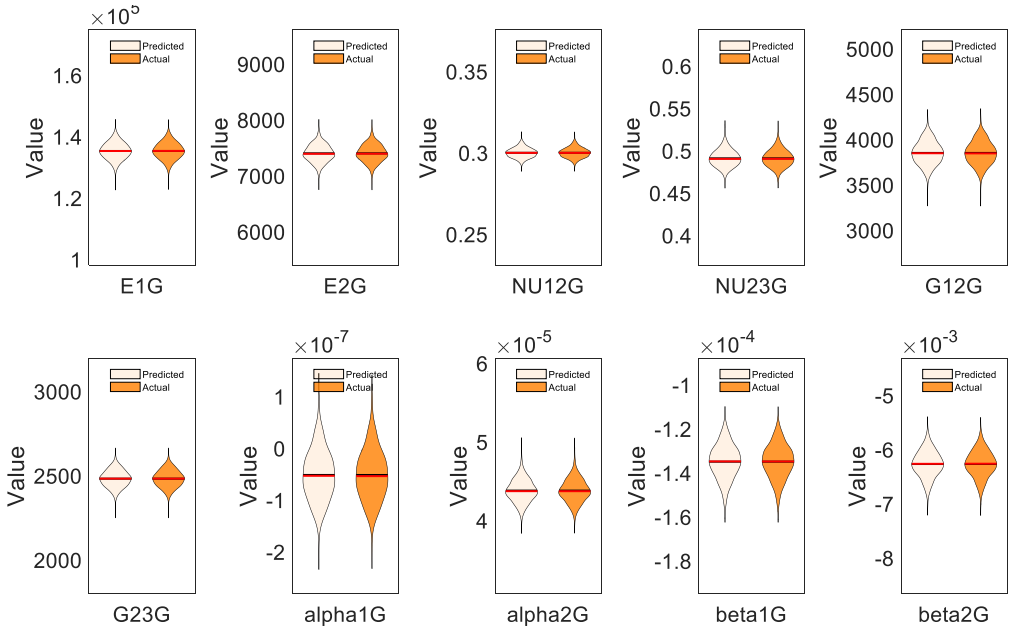

(b)

Figure 9. Output variation prediction and comparison (microscale). (a) Rubbery state variables; (b) Glassy state variables.

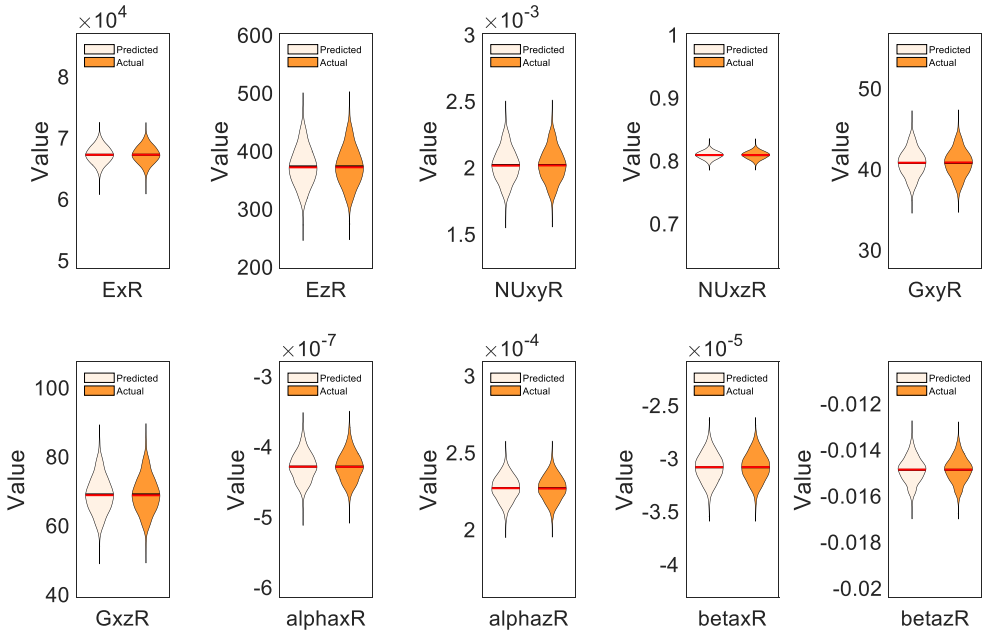

(a)

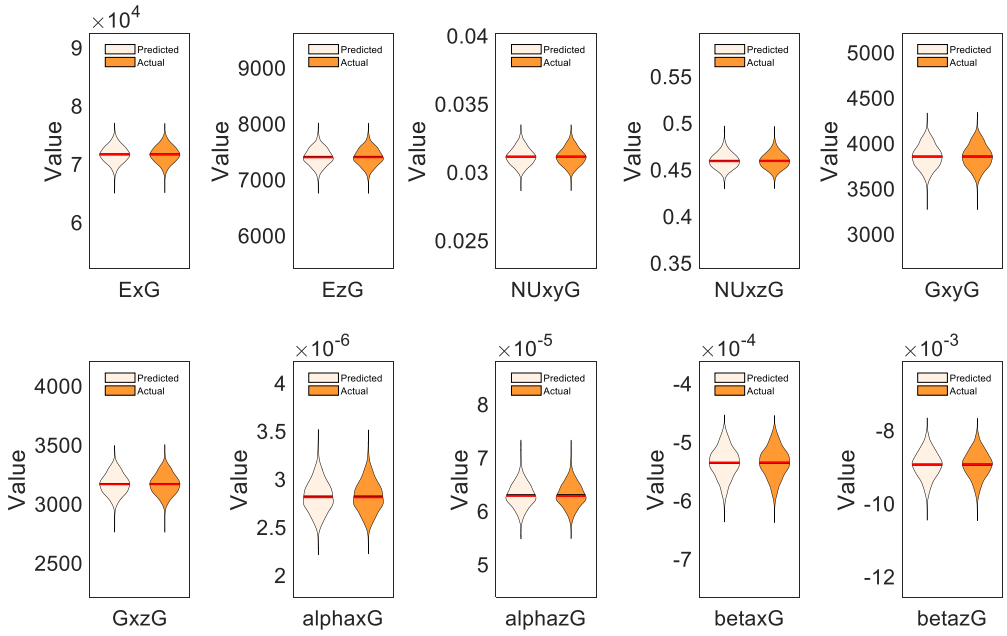

(b)

Figure 10. Output variation prediction and comparison (mesoscale). (a) Rubbery state variables; (b) Glassy state variables.

The hierarchical computational framework developed in this research is flexible, as it can enable the UQ analysis with multiple uncertainty sources at different scales. Such UQ analysis therefore is of the nested nature, in which the top-down sampling strategy can be used to produce the uncertainty samples (Bostanabad et al, 2018). Due to the curse of dimensionality, meta-modeling technique appears to be the only solution to facilitate the nested UQ analysis. In this case, we additionally introduce 2% variations of physical properties at both microscale and mesoscale to produce 1,000 uncertainty samples correspondingly following the procedures outlined in Section 3.2. With nested Monte Carlo simulation, the spring-in angle variation is characterized upon the product of numbers of uncertainty samples at different scales, i.e., $1,000^3$. The spring-in angle distribution of nested UQ analysis is shown in Figure 11b. For comparison, the original spring-in angle distribution shown in Figure 11a is added as a baseline. While the distributions overall match well, certain difference can be observed, where the distribution of nested UQ analysis exhibits zigzag pattern, illustrating the highly nonlinear relation between the spring-in angle and different uncertainties that are sequentially introduced. This shows the complexity of uncertainty propagation in actual process.

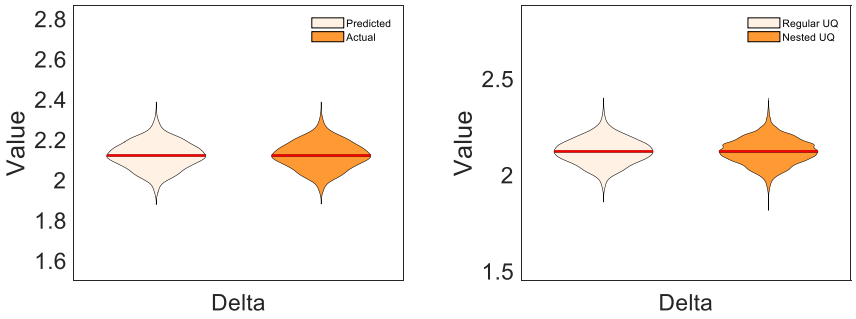

(a) (b)

Figure 11. Spring-in angle variation prediction (macroscale). (a) Comparison of predicted and actual values in regular UQ analysis; (b) Comparison of predicted values in regular and nested UQ analyses.

3.3. UP path importance quantification with Sobol index-based sensitivity matrices

The eventual outcome of this research is to explore the uncertainty propagation within the multi-scale simulation. This is accomplished through the implementation of global sensitivity analysis based on the hierarchical MRGP meta-models established in Section 3.2. Here without loss of generality the first order Sobol indices are taken into account to represent the sensitivity relation of different property variables. By computing all required Sobol indices, we can generate one sensitivity matrix to quantitatively measure the relation of variables at certain two adjacent scales. The number of sensitivity matrices yielded hence is equal to the number of MRGP meta-models. In this study, 5 sensitivity matrices are established to interpret the underlying pattern of uncertainty propagation (UP), as shown in Figure 12. The sensitivity degree is reflected by the color darkness for visualization purpose.

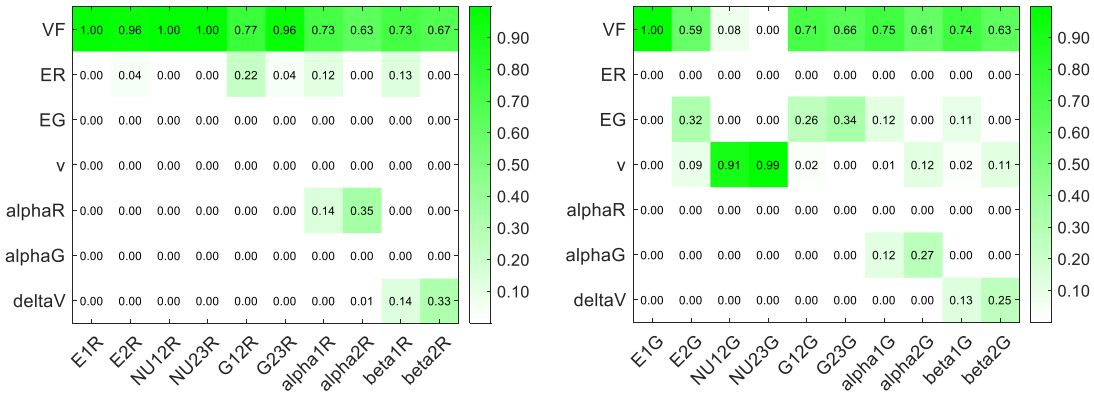

(a) (b)

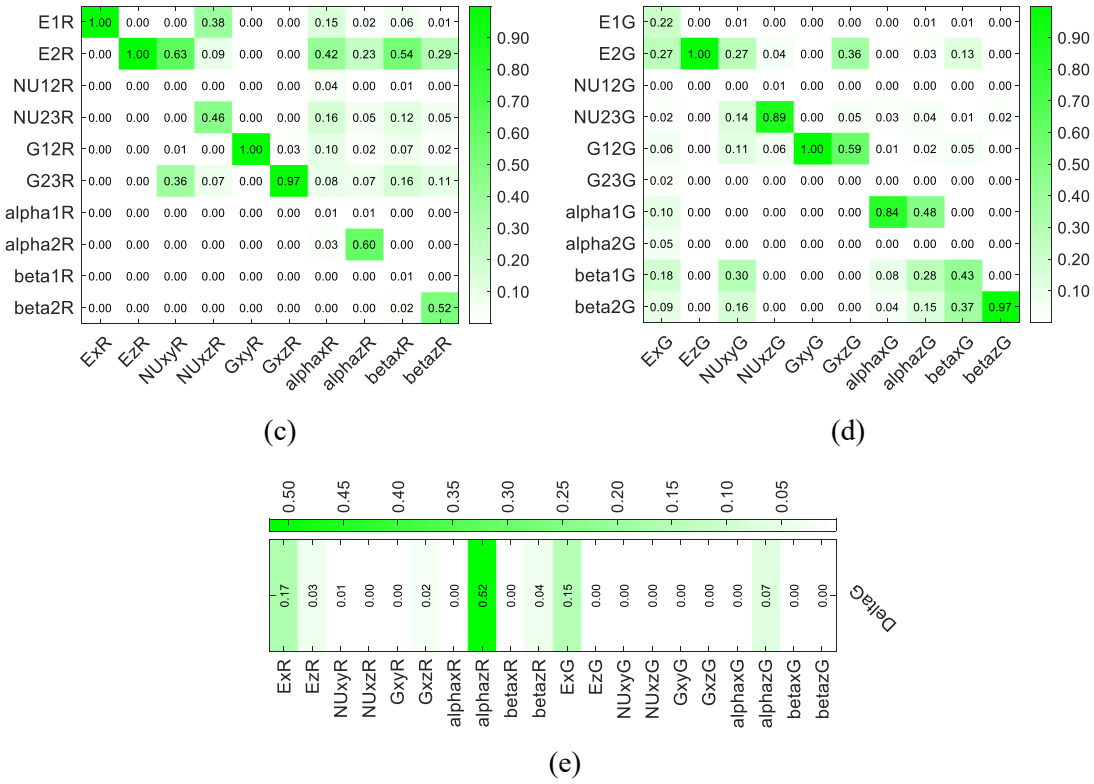

Figure 12. Sobol sensitivity matrices for establishing UP network. (a) Uncertainties versus rubbery state properties at microscale; (b) Uncertainties versus glassy state properties at microscale; (c) Rubbery state properties at microscale versus rubbery state properties at mesoscale; (d) Glassy state properties at microscale versus glassy state properties at mesoscale; (e) Properties at mesoscale versus spring-in angle at macroscale.

As can be seen in Figures 12a and 12b, fiber volume fraction V_f (or 'VF') affects nearly all physical properties at the microscale, especially for the properties in the rubbery state. This is due to the fact that in a continuous, long fiber-reinforced composites, the fiber and matrix have distinct thermo-mechanical properties. The difference is more significant when the matrix is in the rubbery state. This observation is also consistent with the findings reported in literature, where it was found that the fiber volume fraction is significantly influential to the part deformation and mechanical properties in curing process (Parmentier et al, 2016; Singh et al, 2020). Other uncertainty variables generally show less significant contributions. The physical properties at the microscale primarily impact their counterparts at the mesoscale (Figures 12c and 12d), as the large index values occur at diagonal lines of sensitivity matrices. The thermal expansion coefficients and Young's moduli at the mesoscale exhibit relatively larger impacts than others to the spring-in angle (Figure 12e). Among them, the thermal expansion coefficient 'alphazR' in the rubbery state plays

the most important role. The reason is that, the thermal expansion coefficient essentially reflects the degree of material deformation with respect to the temperature, which undoubtedly is critical to the spring-in angle of composite. The contribution of the glassy state Young's modulus, i.e., ' ExG ' is also notable.

In this UP network, each complete path is the route that starts from the first level with raw material uncertainties and terminates at the last level with spring-in angle variation. For example, as shown in Figure 2, $E_m^R \to E_{1G} \to E_{xG} \to \delta_G$ is a complete UP path. The UP network in this study has a total of 1,400 paths. The indicator to quantify the importance of each complete UP path is formulated as

$$\ell_{i,j,k,o} = \frac{\gamma_{i,j,k,o}}{\sum_{i=1}^{I}\sum_{j=1}^{J}\sum_{k=1}^{K}\sum_{o=1}^{O}\gamma_{i,j,k,o}} \tag{19}$$

where $\gamma_{i,j,k} = S^{(1)}_{1i\to 2j} S^{(1)}_{2j\to 3k} S^{(1)}_{3k\to 4o}$. $\ell_{i,j,k,o}$ is a normalized path significance indicator. $S^{(1)}_{\cdot}$ denotes the first order Sobol index of a particular input with respect to the related output. *I*, *J*, *K* and *O* respectively denote the numbers of physical variables at raw material level, spatial microscale, mesoscale and macroscale, respectively.

According to Equation (19), we can compute the indicator values of all paths in the UP network, and further identify the most significant 10 paths as demonstrated in Figure 13. The indicator values of these 10 paths are shown in the right side of the figure. From the result, it is clearly observed that the major uncertainty propagation takes place at the top of the network, which points to the composite process during rubbery state. The most important paths always start from fiber volume fraction in resin. Young's moduli and thermal coefficients appear to be very significant intermediate stations for uncertainty propagation. Specifically, the thermal coefficient ' alphazR ' has the most important influence on the uncertainty propagation because 5 top paths are all associated with this property. As the path importance analysis is built upon the sensitivity matrices, the outcome of this UP analysis here essentially is the consequence of the results shown in Figure 11. Such analysis outcome can provide the qualitative understanding and guideline for the future process design and control. For example, one may notice that top 4 paths contribute more than 50% of total importance to uncertainty propagation. In those paths, the fiber volume fraction, Young's moduli and thermal coefficients are frequently occurred, which require the special attention/care in actual process. Intuitively, we need to find the related process conditions/parameters that can be potentially tuned to minimize the variations of those significant properties, thereby maintaining the finished composite with consistently good quality, i.e., small spring-in angle. Nevertheless, to conduct the process design and control in a quantitative manner, the mathematically rigorous optimization analysis needs to be carried out, which is subject to the future research. The major contribution of this research is to deliver a generic numerical platform for quantifying the interrelationship of hidden properties within the complex

process that is hierarchical in nature. It is worth noting that the top-down multi-scale simulation is a prevailing approach to unravel the mechanism behind many types of manufacturing processes, such as nano manufacturing (Yang et al,2009), and laser power bed fusion additive manufacturing (Zhang et al, 2018; Moser et al, 2019), etc. Therefore, our framework can be extended into those potential manufacturing processes for uncertainty analysis.

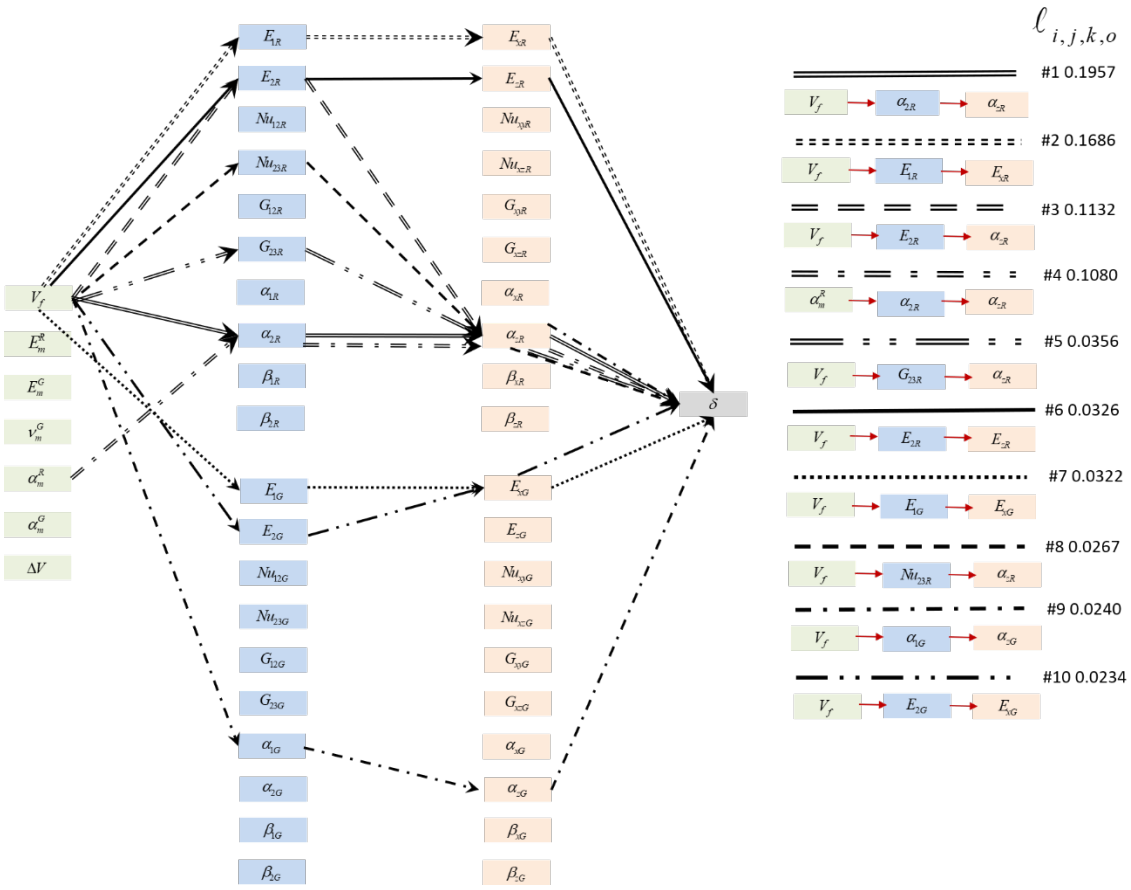

Figure 13. UP path importance identified.

4. Concluding remarks

In this research, a hierarchical computational framework comprised of the multiple multi-response Gaussian process (MRGP) meta-models is established to facilitate uncertainty analysis of multi-scale composite process simulation. Once trained, the MRGP meta-models are capable of efficiently predicting physical properties of interest at different scales, and meanwhile capturing their inherent correlations. This framework supports the nested uncertainty quantification analysis, allowing the analysis of consequences of multiple uncertainty sources at different scales. Furthermore, a global sensitivity analysis is conducted to build a quantitative sensitivity-based uncertainty propagation network, in which the importance of all propagation paths can be assessed. The effectiveness of this new framework is illustrated through

comprehensive case studies. The results obtained offer the guidelines and insights for future experimental design and process control. The developed numerical platform is generic, which can be applied into the uncertainty analysis of other manufacturing processes.

Acknowledgment

This research is supported by AFRL Materials and Manufacturing Directorate (AFRL/RXMS) under contract FA8650-18-C-5700.

Data availability

The raw data required to build the curing model and the processed data used to generate the spring-in angle variability will be available in cdmHUB (cdmhub.org) once the manuscript is accepted.

References

Arendt, P.D., Apley, D.W., and Chen, W., 2012a, "Quantification of model uncertainty: calibration, model discrepancy, and identifiability," Transaction of ASME Journal of Mechanical Design, 134(10), 100908.

Arendt, P. D., Apley, D. W., Chen, W., Lamb, D., and Gorsich, D., 2012b, "Improving identifiability in model calibration using multiple responses," Transaction of ASME Journal of Mechanical Design, 134(10), 100909.

Au, S.K., and Beck, J.l., 2003, "Subset simulation and its application to seismic risk based on dynamic analysis," Journal of Engineering Mechanics, 129(8): 901-917.

Bostanabad, R., Liang, B., Gao, J., Liu, W.K., Cao, J., Zeng, D., Su, X., Xu, H., Li, Y., and Chen W., "Uncertainty quantification in multiscale simulation of woven fiber composites," Computer Methods in Applied Mechanics and Engineering, 338: 506-532.

Balokas, G., Czichon, S., and Rolfes, R., 2018, "Neural network assisted multiscale analysis for the elastic properties prediction of 3D braided composites under uncertainty," Composite Structures, 183(1): 550-562.

Chen, W., 2019, An Integrated Flow-Curing Model for Predicting Residual Stresses in Textile Composites in Textile Composites Ph.D. thesis University of Connecticut.

Chen, W., and Zhang, D., 2018, "A micromechanics-based processing model for predicting residual stress in fiber-reinforced polymer matrix composites," Composite Structures, 204:153-66.

Chen, X., and Qiu, Z., 2018, "A novel uncertainty analysis method for composite structures with mixed uncertainties including random and interval variables," Composite Structures, 184: 400-410.

Dai, H., Zheng, Z., and Ma, H., 2019, "An explicit method for simulating non-Gaussian and non-stationary stochastic processes by Karhunen-Loeve and polynomial chaos expansion," Mechanical Systems and Signal Processing, 115, pp:1-13.

Daniel, I.M., and Ishai, O., *Engineering Mechanics of Composite Materials*, Oxford University Press, 2006.

Ding, A., Li, S., Wang, J., and Zu, L., 2015, "A three-dimensional thermo-viscoelastic analysis of process-induced residual stress in composite laminates," Composite Structures, 129:60-69.

Du, A., and Padgett, J.E., 2020, "Investigation of multivariate seismic surrogate demand modeling for multi-response structural systems," Engineering Structures, 207, 110210.

Draper, N. R., and Smith, H., *Applied Regression Analysis*, Wiley-Interscience, 1998.

Efron, B., and Stein, C., 1981, "The jacknife estimate of variance," The Annals of Statistics, 9:586-596.

Ersoy, N., Grstka, T., Potter, K., Wisnom, M.R., Porter, D., Clegg, M., and Stringer, G., 2010, "Development of the properties of a carbon fibre reinforced thermosetting composite through cure," Composites Part A: Applied Science and Manufacturing, 41(3):401-409.

Gallager, R.G., *Stochastic Processes: Theory for Applications*, Cambridge University Press, 2013.

Ghanem, R., Higdon, D., and Owhadi, H., *Handbook of Uncertainty Quantification*, Springer, 2017.

Grover, N., Sahoo, R., Singh, B.N., and Maiti, D.K., 2017, "Influence of parametric uncertainties on the deflection statistics of general laminated composite and sandwich plates," Composite Structures, 171(1):158-169.

Heinrich, C., Aldridge, M., Wineman, A.S., Kieffer, J., Waas, A.M., and Shahwan K.W., 2013, "The role of curing stresses in subsequent response, damage and failure of textile polymer composites," Journal of the Mechanics and Physics of Solids, 61(5):1241-64.

Helton, J.C., and Davis, F.J., 2003, "Latin hypercube sampling and the propagation of uncertainty in analyses of complex systems," Reliability Engineering & System Safety, 81(1): 23-69.

Homma, T., and Saltelli, A., 1996, "Importance measures in global sensitivity analysis of nonlinear models," Reliability Engineering and System Safety, 52(1):1-17.

Hubert P., Johnston A., Poursartip A., and Nelson K., 2001, "Cure kinetics and viscosity models for Hexcel 8552 epoxy resin," International SAMPE Symposium and Exhibition, 46: 2341-54.

Khristenko, U., Constantinescu, A., Tallec, P.L.E., Tinsley Oden, J., and Wohlmuth, B., 2020, "A statistical framework for generating microstructures of two-phase random materials: application to fatigue analysis," Multiscale Modeling and Simulation, 18(1):21-43.

Iooss, B., and Lemaitre, P., 2015, "A review on global sensitivity analysis methods," Operations Research/Computer Science Interfaces Series, 59:101-122.

Li, M., and Wang, Z., 2018, “Confidence-driven design optimization using Gaussian process metamodeling with insufficient data,” Journal of Mechanical Design, Transactions of the ASME, 140(2), 121405.

Liu, H., Ong, Y.-S., Shen, X., and Cai, J., 2018, “When Gaussian Process Meets Big Data: A Review of Scalable GPs,” arXiv preprint arXiv:1807.01065.

Marrel, A., Iooss, B., Laurent, B., and Roustant, O., 2009, “Calculation of Sobol indices for the Gaussian process metamodel,” Reliability Engineering and System Safety, 94(3):742-751.

Medina, J.C., and Taflanidis, A.A., 2014, “Adaptive importance sampling for optimization under uncertainty problems,” Computer Methods in Applied Mechanics and Engineering, 279:133-162.

Mehrez, L., Fish, J., Aitharaju, V., Rodgers, W.R., and Ghanem, R., 2018, “A PCE-based multiscale framework for the characterization of uncertainties in complex systems,” Computational Mechanics,61:219-236.

Mesogitis, T.S., Skordos, A.A., and Long, A.C., 2014, “Uncertainty in the manufacturing of fibrous thermosetting composites: a review,” Composites Part A: Applied Science and Manufacturing, 57:67-75.

Moser, D., Cullinan, M., and Murthy, J., 2019, “Multi-scale computational modeling of residual stress in selective laser melting with uncertainty quantification,” Additive Manufacturing, 29, 100770.

Parmentier, A., Wucher, B., and Dumas, D., 2016, “Influence of the fibre volume fraction parameter on the predictions of the cure-induced deformations in thermoset composite parts,” Proceeding of the 17th European Conference on Composite Materials, ECCM2016, 126913.

Peng, X., Li, D., Wu, H., Liu, Z., Li, J., Jiang, S., and Tan, J., 2019, “Uncertainty analysis of composite laminated plate with data-driven polynomial chaos expansion method under insufficient input data of uncertainty parameters”, Composite Structures, 209:625-633.

Rasmussen, C.E., and Williams, C.K., *Gaussian Processes for Machine Learning*, The MIT Press, 2006.

Refaeilzadeh P., Tang L., and Liu H., *Cross-Validation. Encyclopedia of Database Systems.* Springer, Boston, MA, 1998.

Saltelli, A., 2002, “Making best use of model evaluations to compute sensitivity indices,” Computer Physics Communication, 145:280-297.

Schueller, G.I., 2009, “Efficient monte carlo simulation procedures in structural uncertainty and reliability analysis - recent advances,” Structural Engineering and Mechanics, 32(1):1-20.

Shields, M.D., and Zhang, J., 2016, “The generalization of Latin hypercube sampling,” Reliability Engineering & System Safety, 148:96-108.

Singh, J.I.P, Singh, S., and Dhawan, V., 2020, “Influence of fiber volume fraction and curing temperature on mechanical properties of jute/PLA green composites,” Polymers and Polymer Composites, 128(4):273-284.

Soize, C., 2010, “Identification of high-dimension polynomial chaos expansions with random coefficients for non-Gaussian tensor-valued random fields using partial and limited experimental data,” Computer Methods in Applied Mechanics and Engineering, 199(33-36), pp:2150-2164.

Tavakol, B., Roozbehjavan, P., Ahmed, A., Das, R., Joven, R., Koushyar, H., Rodriguez, A., Minaie, B., 2013, “Prediction of residual stresses and distortion in carbon fiber-epoxy composite parts due to curing process using finite element analysis,” Journal of Applied Polymer Science, 128(2)941-950.

Wan, H.P., Mao, Z., Todd, M.D., and Ren, W.X., 2014, “Analytical uncertainty quantification for modal frequencies with structural parameter uncertainty using a Gaussian process metamodel,” Engineering Structurs, 75:577-589.

Yang, P., Liao, N.B., and Shang, S.H., 2009, “Multi-scale modeling and numerical analysis of thermal behavior of Cu-Al interface structure in micro/nano manufacturing,” International Journal of Nonlinear Sciences and Numerical Simulation, 10(4):483-491,

Zhang, C.Y., Wang, Z, Fei, C.W., Wei, J.S., and Tang, W.Z., 2019, “Fuzzy multi-SVR learning model for reliability-based design optimization of turbine blades,” Materials, 12(15), 2341.

Zhang, D., and Wass, A.M., 2014, “A micromechanics based multiscale model for nonlinear composites,” Acta Mechanica, 225(4–5):1391–1417.

Zhang, J., Zhang, Y., Lee, W.H., Wu, L., and Choi, H.H., 2018, “A multi-scale multi-physics modeling framework of laser powder bed fusion additive manufacturing process,” Metal Powder Report, 73(3): 151-157.

Zhou, K., and Tang, J., 2017, “Design optimization toward alleviating forced response variation in cyclically periodic structure using Gaussian process,” Transactions of ASME Journal of Vibration and Acoustics, 139(1), 011017.

Zhou, K., and Tang, J., 2018, “Uncertainty quantification in structural dynamic analysis using two-level Gaussian processes and Bayesian inference,” Journal of Sound and Vibration, 412:95-115.

Zhou, K., and Tang, J., 2021a, “Uncertainty quantification of mode shape variation utilizing multi-level multi response Gaussian process,” Transaction of ASME Journal of Vibration and Acoustics, 143(1): 011003.

Zhou, K., and Tang, J., 2021b, “Structural model updating using adaptive multi-response Gaussian process meta-modeling,” Mechanical Systems and Signal Processing, 147, 107121.